Heparan sulfate and heparanase play key roles in mouse β cell survival and autoimmune diabetes

Andrew F. Ziolkowski, Sarah K. Popp, Craig Freeman, Christopher R. Parish, and Charmaine J. Simeonovic

Department of Immunology, The John Curtin School of Medical Research, The Australian National University, Canberra, Australia.

The autoimmune type 1 diabetes (T1D) that arises spontaneously in NOD mice is considered to be a model of T1D in humans. It is characterized by the invasion of pancreatic islets by mononuclear cells (MNCs), which ultimately leads to destruction of insulin-producing β cells. Although T cell dependent, the molecular mechanisms triggering β cell death have not been fully elucidated. Here, we report that a glycosaminoglycan, heparan sulfate (HS), is expressed at extraordinarily high levels within mouse islets and is essential for β cell survival. In vitro, β cells rapidly lost their HS and died. β Cell death was prevented by HS replacement, a treatment that also rendered the β cells resistant to damage from ROS. In vivo, autoimmune destruction of islets in NOD mice was associated with production of catalytically active heparanase, an HS-degrading enzyme, by islet-infiltrating MNCs and loss of islet HS. Furthermore, in vivo treatment with the heparanase inhibitor PI-88 preserved intraislet HS and protected NOD mice from T1D. Our results identified HS as a critical molecular requirement for islet β cell survival and HS degradation as a mechanism for β cell destruction. Our findings suggest that preservation of islet HS could be a therapeutic strategy for preventing T1D.

Introduction

The NOD mouse strain spontaneously develops autoimmune type 1 diabetes (T1D) and is recognized as an experimental model for T1D in humans. The disease develops slowly in NOD mice, and the autoimmune pathology initially involves a nondestructive insulitis (NDI), in which mononuclear cells (MNCs) accumulate around the periphery of the islets. Autoimmune destruction of insulin-producing pancreatic β cells and T1D occurs when the insulitis MNCs become destructive and invade the islets (1). The trigger for this conversion is unknown. Although autoimmune diabetes in NOD mice is T cell dependent, it is unclear how β cells are destroyed once autoreactive T lymphocytes have entered the islets. Evidence suggests that CD8+ T cells recognize peptides derived from β cell–specific autoantigens (including proinsulin/insulin, GAD, IGRP, and chromogranin A) in the context of class I MHC molecules on the cell surface and kill the β cells via the perforin/granzyme pathway of cytotoxicity or induce apoptosis by Fas/FasL signaling (2–7). CD4+ T cells activated by autoantigen peptide/class II MHC complexes on intraislet APCs are likely to amplify islet inflammation by producing nonspecific inflammatory mediators, such as cytokines and chemokines. Intraislet APCs activated in the cytokine milieu could also indirectly damage β cells by producing ROS or cytokines that induce endogenous production of free radicals in the β cells (3).

Intervention therapies have been developed to impede the inflammatory response to islets in NOD/Lt mice. mAb treatment targeting CD4+ or CD3+ T cells has been particularly effective in preventing the development of T1D (8, 9). In the case of anti-CD4 mAb therapy, continual treatment was mandatory and induced

CD4+ T cell depletion (9). Anti-CD3 mAb therapy rescued NOD mice from T1D, even when treatment was delayed until after T1D onset, and restored self tolerance after only transient T cell depletion (10). Other experimental therapies targeting cytokines including IL-16, IL-21, and TNF inhibited the recruitment of diabetogenic T cells to the pancreas, reduced insulitis, and prevented T1D (11–13). NOD islets in situ produce chemokines, particularly CCL5 (14), that recruit inflammatory cells, which suggests that β cells themselves could contribute to the initiation and expansion of peri-islet insulitis. Blockade of chemokine signaling via transgenic expression of a chemokine-blocking protein or decoy receptor by β cells has markedly decreased insulitis and T1D incidence in NOD mice (15, 16). Despite the development of effective strategies for reducing insulitis and preventing T1D in NOD mice, practical problems have impeded their clinical application. Notably, recent clinical trials have revealed inconsistent improvement in T1D control after anti-CD3 therapy, and long-term protection from disease progression remains an elusive milestone (17).

Intrinsic properties of β cells have been identified that render them particularly vulnerable to inflammatory insult. In addition to their capacity to secrete chemokines that could exacerbate peri-islet inflammation, islet β cells express low levels of free radical scavenger enzymes, potentially increasing their sensitivity to free radical–mediated damage (18). Conversely, the extent to which islets and β cells use intrinsic defense and survival mechanisms for their protection has largely been underexplored. We recently reported that in situ NOD mouse islets are surrounded by a continuous basement membrane (BM) containing the heparan sulfate proteoglycan (HSPG) perlecan (19). HSPGs consist of a core protein to which a number of side-chains of the glycosaminoglycan or complex sugar heparan sulfate (HS) are covalently attached. HS is a linear polysaccharide consisting of repeating disaccharides of glucosamine and glucuronic acid; there are large regions of N-acetylglucosamine and glucuronic
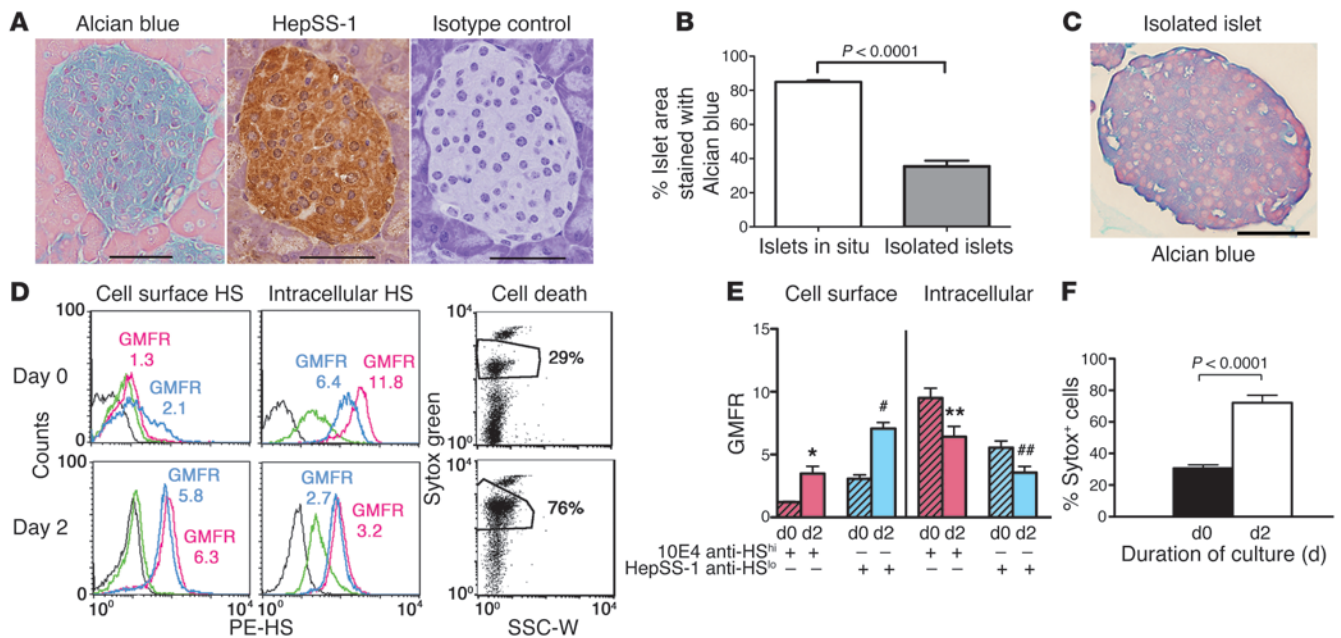
Figure 1

HS is highly expressed within pancreatic islets in situ, and HS loss in vitro correlates with β cell death. (**A**) Detection of HS in NOD/SCID pancreatic islets in situ by Alcian blue histochemistry and immunohistochemistry using HepSS-1 anti-HS mAb. No background staining with isotype control mouse IgM was observed. Scale bars: 50 μm. (**B**) Intra-islet HS content (quantified by Image J with Color Deconvolution plugin) showed that the area of intraislet staining with Alcian blue was significantly higher in islets in situ ($n = 50$) than after isolation ($n = 45$; $P < 0.0001$). (**C**) Isolated BALB/c islet showing loss of intraislet HS by Alcian blue staining. Scale bar: 50 μm. (**D**) Intracellular HS staining was further reduced in BALB/c islet β cells during culture, as demonstrated by FACS staining using HepSS-1 (anti-HS^{lo}; blue histogram) and 10E4 (anti-HS^{hi}; pink histogram) mAbs or an isotype control IgM (green histogram); black histogram denotes islet cell autofluorescence. Loss of β cell viability after culture for 2 days, as measured by Sytox green uptake (dead/dying cells), is shown at right. SSC-W, side scatter width. (**E**) Loss of intracellular HS^{hi} and HS^{lo} and increase of cell surface HS^{hi} and HS^{lo} was seen in β cells cultured for 2 days. *$P = 0.0022$; #$P < 0.0001$; **$P = 0.0225$; ##$P = 0.0202$. (**F**) Loss of intracellular HS during culture for 2 days, as in **E**, correlated with a significant increase in percent Sytox green+ β cells ($P < 0.0001$). Data are mean ± SEM ($n = 6$).

acid interspersed with small regions containing sulfated glucosamine and iduronic acid residues. Although regions of the HS chains are characteristically sulfated, their chemical structure shows additional heterogeneity, varying in the position of O- and N-sulfation and in epimerization of glucuronic acid to iduronic acid (20, 21). HSPGs in extracellular matrices (ECMs) and on the surface of cells act as reservoirs for growth factors, cytokines, and chemokines. However, when localized in BMs, HSPGs have the additional function of obstructing cell migration (20). This property suggests that the islet BM containing the HSPG perlecan would constitute a primary defense mechanism against invasion by destructive insulitis (DI) MNCs.

To migrate to sites of inflammation, such as peri-islet insulitis in the pancreas, leukocytes need to first extravasate from blood vessels and then produce a panel of degradative enzymes to solubilize the matrix components of the subvascular endothelial BM. Of these, heparanase (encoded by *HPSE*) plays a particularly critical role because it is the only known mammalian endoglycosidase that can efficiently degrade the HS side-chains of HSPGs (20, 22). In support of this, inhibition of heparanase using sulfated oligosaccharides or modified heparins has been shown to prevent inflammation and limit metastasis of experimental tumors (20, 22). Likewise, we have previously observed that MNC entry into islets, which marks the onset of destructive autoimmunity in NOD mice, correlates with degradation of the islet BM (19).

However, to our knowledge, a role for heparanase in the repertoire of effector molecules produced by insulitis MNCs has not previously been investigated.

In this study, we report that a protective role for HS extends beyond that of the islet BM (19). We observed remarkably high levels of HS in normal islets in situ, primarily as a result of its unusual intracellular localization within islet β cells. In vitro, we showed that HS functioned as an important survival mechanism for β cells, with loss of β cell HS representing a mechanism of β cell death. Surprisingly, HS replacement provided protection from free radical–mediated cell death. We showed that in vivo, destructive autoimmunity was associated with degradation of islet HS by heparanase produced by insulitis MNCs and was prevented by administration of a heparanase inhibitor. We therefore identify endogenous HS as a β cell target for autoimmune damage, with heparanase as a mediator of β cell autoimmunity, findings we believe to be novel. Our results suggest that heparanase inhibition may be a promising therapeutic strategy for protecting β cells from HS depletion and T1D progression.

Results

HS is highly expressed in mouse islets in situ. While investigating the HS content of pancreatic islet BMs, we identified remarkably high levels of intracellular HS within the islets of conventional mouse strains, young NOD mice, and immunoincompetent NOD/SCID
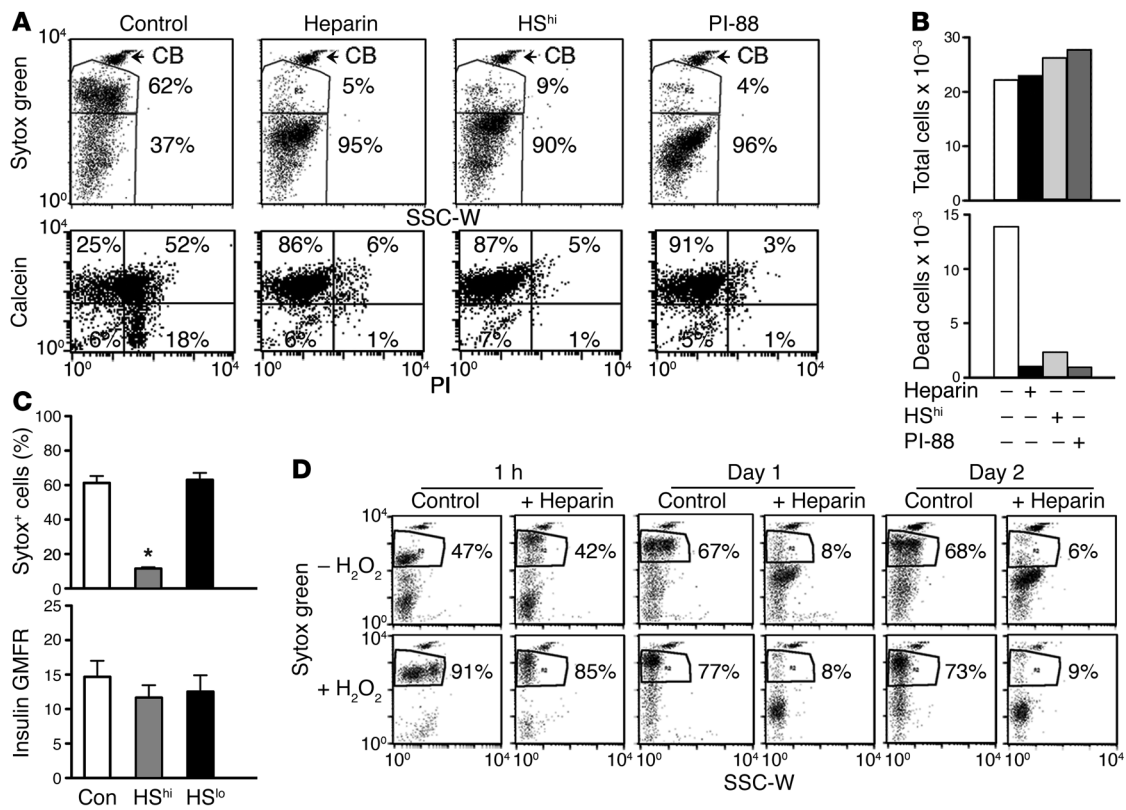
Figure 2

HS replacement protects isolated β cells from culture-induced and ROS-induced cell death in vitro. (**A**) Flow cytometry analysis of isolated β cell viability after culture for 2 days in the absence (control) or presence of 50 μg/ml heparin, HS[hi], or PI-88. Viability was assessed by Sytox green uptake or by calcein-AM (viable and apoptotic cells) and PI (dead and apoptotic cells) uptake (see Supplemental Table 1). CB, counting beads. Percent cells is shown for the respective regions. (**B**) Absolute number of β cells and number of dead β cells in 2 day cultures as in **A**. The number of β cells was calculated using counting beads. See Supplemental Table 1 for statistical analyses of the same day 2 cultures (note that percent Sytox green^{+} cells approximated percent PI^{+} cells). (**C**) Coculture with HS[hi], but not HS[lo], protected isolated islet β cells from 2 day culture–induced cell death, as determined by percent Sytox green^{+} cells and intracellular insulin staining of β cells. GMFR for insulin staining was compared with serum control. *$P < 0.05$ vs. control. (**D**) Ability of β cells cultured in the presence or absence of heparin (50 μg/ml) for 1 hour or 1–2 days to resist H_2O_2-induced (i.e., ROS) cell death (see Table 1). Data in **A** and **D** are representative of 3–5 separate experiments.

mice (Figure 1A), using immunohistochemistry and also HS-specific histochemical staining by Alcian blue (23). Staining of islets with Alcian blue was abolished by prior treatment of pancreas tissue sections with nitrous acid, a procedure that cleaves the N-sulfated glucosamines found only in HS, but not the N-acetylated glucosamines present in other glycosaminoglycans (refs. 24, 25, and Supplemental Figure 1; supplemental material available online with this article; doi:10.1172/JCI46177DS1). The direct detection methods we used to localize HS in islets represent a technical advance over the indirect approach of identifying HS "stubs" after heparitinase treatment of pancreas sections (26).

Loss of HS from β cells in vitro correlates with β cell death. Compared with islets in situ in the pancreas, Alcian blue histochemistry showed the HS content of islets was significantly reduced by more than 50% after their isolation in vitro (Figure 1, B and C). After enzymatic dispersion of the islets to single-cell suspensions, flow cytometry analyses showed that the isolated β cells stained for both highly sulfated HS (HS[hi]; identified by the 10E4 mAb) and undersulfated HS (HS[lo]; identified by the HepSS-1 mAb), but the remaining HS was localized mainly intracellularly, with low levels of HS present on the cell surface (Figure 1D). Furthermore, the

majority of isolated islet cells were insulin-positive β cells (Supplemental Figure 2). Cell surface HS was significantly increased 2- to 3-fold, and intracellular HS was significantly decreased to 67% of preculture levels after 2 days of culture (Figure 1, D and E), which suggests that cell surface HS may be replenished from intracellular HS stores. The loss of intracellular HS during culture was accompanied by a substantial (>2-fold) increase in β cell death, as determined by uptake of Sytox green, a DNA dye that stains dead and dying cells (Figure 1, D and F). These findings suggested that β cells may require intracellular HS for their survival.

HS replacement protects isolated β cells from culture- and ROS-induced cell death. In support of the notion that HS is needed for β cell survival, β cells were prevented from dying in culture after the addition of 50 μg/ml heparin, a highly sulfated analog of HS, to the culture medium (Figure 2, A and B, and Table 1). The viability of β cells after 2 days of culture with heparin was 95%, compared with 37% viability in control cultures, based on Sytox green exclusion (Figure 2A). The low cell viability in the control cultures is probably related to the culture conditions, in which dispersed islet cells adhered to the nontreated plastic surface of the wells (see Methods). This remarkable heparin-induced improvement in viability

Table 1
Heparin protects mouse β cells from culture- and ROS-induced cell death

Culture	ROS	Sytox green+ β cells (%)		
		1 hour	1 day	2 days
Control	None	35.5 ± 4.2	66.3 ± 1.7	67.0 ± 2.3
Control	H₂O₂	88.5 ± 1.0[A]	72.5 ± 2.7	68.3 ± 5.4
Heparin	None	28.5 ± 5.1	7.0 ± 1.1[A]	6.8 ± 1.3[A]
Heparin	H₂O₂	83.5 ± 2.6[B]	10.8 ± 1.1[C]	8.0 ± 1.1[C]

β cells were cultured in the presence or absence of 50 μg/ml heparin for 1 hour, 1 day, or 2 days and then treated or not with 30% H_2O_2 (as a source of ROS) for 5 minutes. Sytox green uptake was used to assess percent cell death by flow cytometry ($n = 4$ per group). [A]$P < 0.05$ vs. untreated control culture. [B]$P < 0.05$ vs. untreated heparin culture. [C]$P < 0.05$ vs. H_2O_2-treated control culture.

was confirmed by uptake of calcein-AM, a fluorescent dye that labels viable and apoptotic cells, and by staining with propidium iodide (PI), a DNA-binding dye that labels dead and apoptotic cells. In the presence of heparin, the highly viable calcein+PI– population of β cells was increased from 25% to 86%, the dead population (calcein–PI+) reduced from 18% to 1%, and the apoptotic population (calcein+PI+) decreased from 52% to 6% (Figure 2A). HS^hi and the HS^hi mimetic PI-88 (27, 28), at 50 μg/ml, were just as effective as heparin at promoting β cell survival (Figure 2A and Supplemental Table 1), although only heparin was active at 5 μg/ml (Supplemental Figure 3). All 3 compounds decreased the absolute number of dead β cells by 6- to 14-fold compared with controls, despite comparable total cell numbers in the cultures (Figure 2B). In contrast to HS^hi, treatment with HS^lo did not protect the β cells (Figure 2C). The effect of heparin treatment on β cell viability was also independent of the source of heparin (porcine mucosal or bovine lung; Supplemental Figure 4, A and B) and occurred after continuous culture with heparin for either 1 or 2 days (Figure 2D and Supplemental Figure 4C), or after pulsing with heparin for 1 hour followed by culture for 2 days in the absence of heparin (data not shown). Flow cytometry analyses, together with confocal microscopy, showed that β cell protection correlated with the intracellular localization of considerable amounts of FITC-labeled heparin in 86% of β cells (Supplemental Figure 5).

Importantly, heparin-treated β cells became extraordinarily resistant to ROS-induced death, generated by acute treatment of the cells with H_2O_2. Whereas H_2O_2 treatment of control β cells after 1 hour of culture significantly increased cell death from 35.5% ± 4.2% to 88.5% ± 1.0%, β cells cultured with 50 μg/ml heparin for 1 or 2 days showed excellent viability in the presence of ROS (10.8% ± 1.1% and 8.0% ± 1.1% cell death, respectively; Table 1 and Figure 2D). Similarly, HS^hi and PI-88, but not HS^lo (Supplemental Figure 6), also protected β cells from ROS-induced cell death. These results demonstrated that intracellular uptake of HS^hi mimetics, such as heparin and PI-88, protected β cells from both culture-induced death and death induced by exogenous ROS. This also suggests that culture-induced death of β cells may be mediated by endogenous ROS.

Pancreatic islets are susceptible to damage by heparanase. Isolated islets with residual intraislet HS were examined for their susceptibility to damage by heparanase, the only known mammalian endoglycosidase that can cleave HS (29). Treatment of isolated islets with

20 μg/ml exogenous human heparanase for 24 hours resulted in peripheral islet damage with increased intraislet cell apoptosis (Supplemental Figure 7). In contrast, the same treatment did not induce apoptosis or death of either B16 melanoma cells or L929 fibroblasts (data not shown). While heparanase was therefore not universally toxic for all types of cells, our data strongly suggest that islets are particularly susceptible to heparanase-mediated damage. To investigate the in vivo relevance of this susceptibility, islets undergoing different levels of autoimmune damage in NOD mice were then examined for HS and heparanase expression. We observed by histochemistry that islets lacking insulitis or with NDI contained widespread and well-preserved HS (Figure 3A). In contrast, islets damaged by DI showed extensive disruption of islet HS, as detected by Alcian blue staining, particularly in close proximity to infiltrating MNCs (Figure 3A). Likewise, prediabetic NOD/Lt mice and NOD/Lt mice at diabetes onset showed a significant reduction in islet HS content compared with intact adult NOD/SCID islets (Figure 3B). When islets from prediabetic and onset diabetic NOD/Lt mice were isolated with their associated insulitis MNCs and examined by quantitative real-time RT-PCR for *Hpse* transcripts, we observed a 4- to 5-fold increase in transcripts in these islets compared with young NOD islets with low insulitis and a 6- to 8-fold increase compared with NOD/SCID islets lacking insulitis (Figure 3, C and D). This finding correlated with an approximately 28-fold increase in mRNA for the common leukocyte marker *Cd45* compared with NOD/SCID islets (Figure 3E), which suggests that the increased *Hpse* mRNA expression was derived from insulitis MNCs. This conclusion was confirmed immunohistochemically, with heparanase protein being strongly expressed by DI MNCs (Figure 3F). Heparanase exists as a 65-kDa proenzyme that is proteolytically cleaved to 8-kDa and 48- to 50-kDa polypeptides that dimerize to form the active enzyme (30–32). Western blotting analysis revealed substantially higher levels of the 48-kDa active mouse heparanase in late prediabetic (9–10 weeks of age; 6-fold) and onset-diabetic NOD islets (9-fold) compared with NOD/SCID islets, with prediabetic NOD islets from 7- to 8-week-old mice containing mainly proheparanase (compared with late prediabetic and onset-diabetic NOD islets; Figure 3G). This finding suggests that insulitis MNCs gain the ability to generate enzymatically active heparanase at the same time as they become able to mediate destructive disease. We also noted that CBA/H, NOD/SCID, and young NOD islets contained substantial *Hpse* transcript levels, 20- to 33-fold those of normal CBA/H kidneys (Figure 3D). Heparanase protein was also detected by immunohistochemistry — albeit weakly — at or near the cell surface of islet β cells, with Western blotting indicating low levels of the enzyme, in NOD/SCID islets (Figure 3, F and G). These findings suggest that active heparanase produced by invading insulitis MNCs, but not inactive heparanase endogenously produced within islets, contributes to autoimmune islet β cell damage during T1D development.

Inhibition of heparanase protects NOD mice from destructive autoimmunity and T1D. The sulfated phosphomanno-oligosaccharide PI-88 (Muparfostat; Progen Pharmaceuticals) is a HS mimetic that is a noncleavable competitive inhibitor of heparanase (27, 29) and a potent inhibitor of tumor growth (27) and is in clinical trials as an anticancer drug (33). To test whether heparanase plays a direct role in the development of autoimmune diabetes, we treated 10.5- to 11-week-old prediabetic female NOD mice (presumably exhibiting both NDI and DI) daily with PI-88. Compared with control saline-treated mice, PI-88 treatment significantly delayed development of T1D by
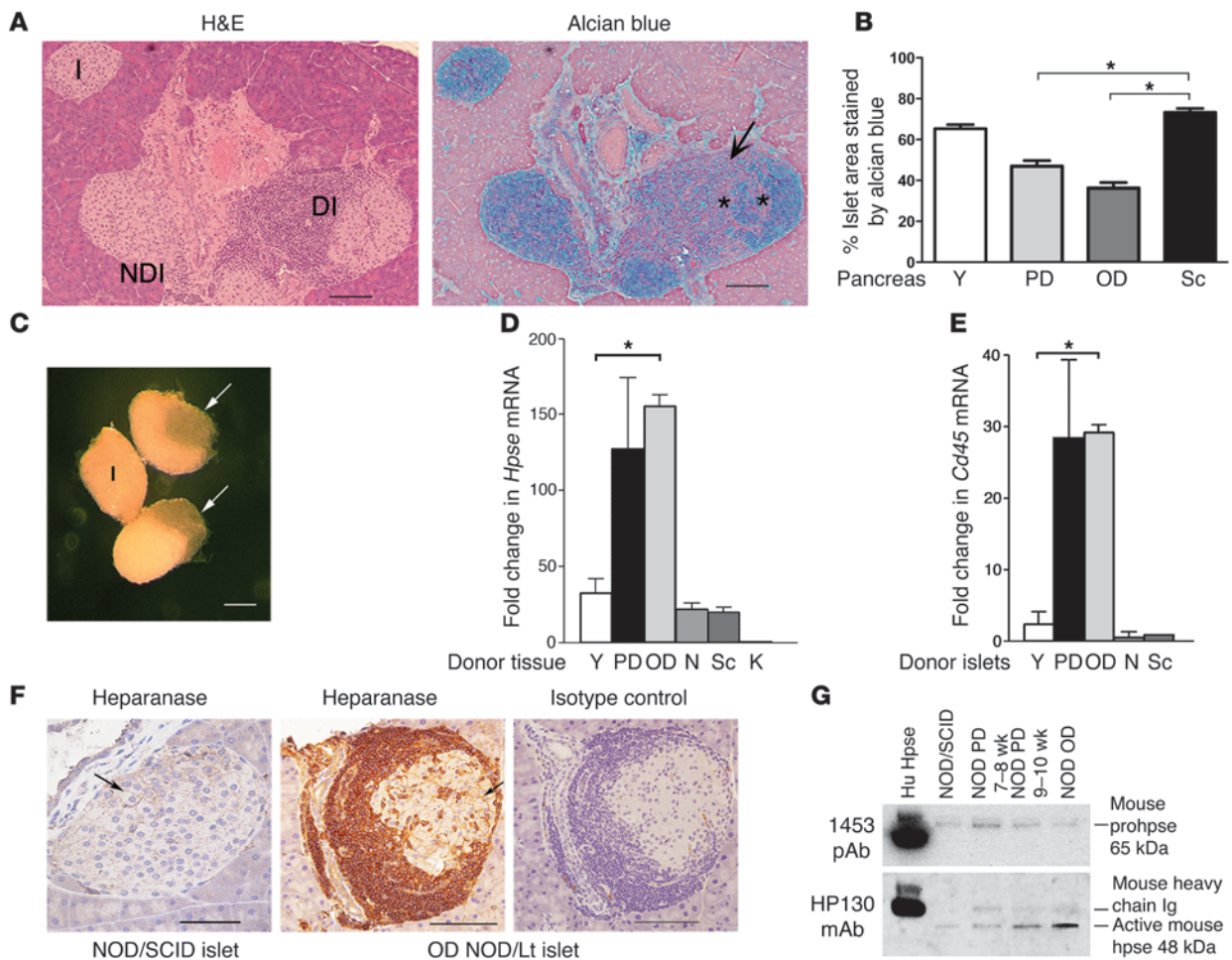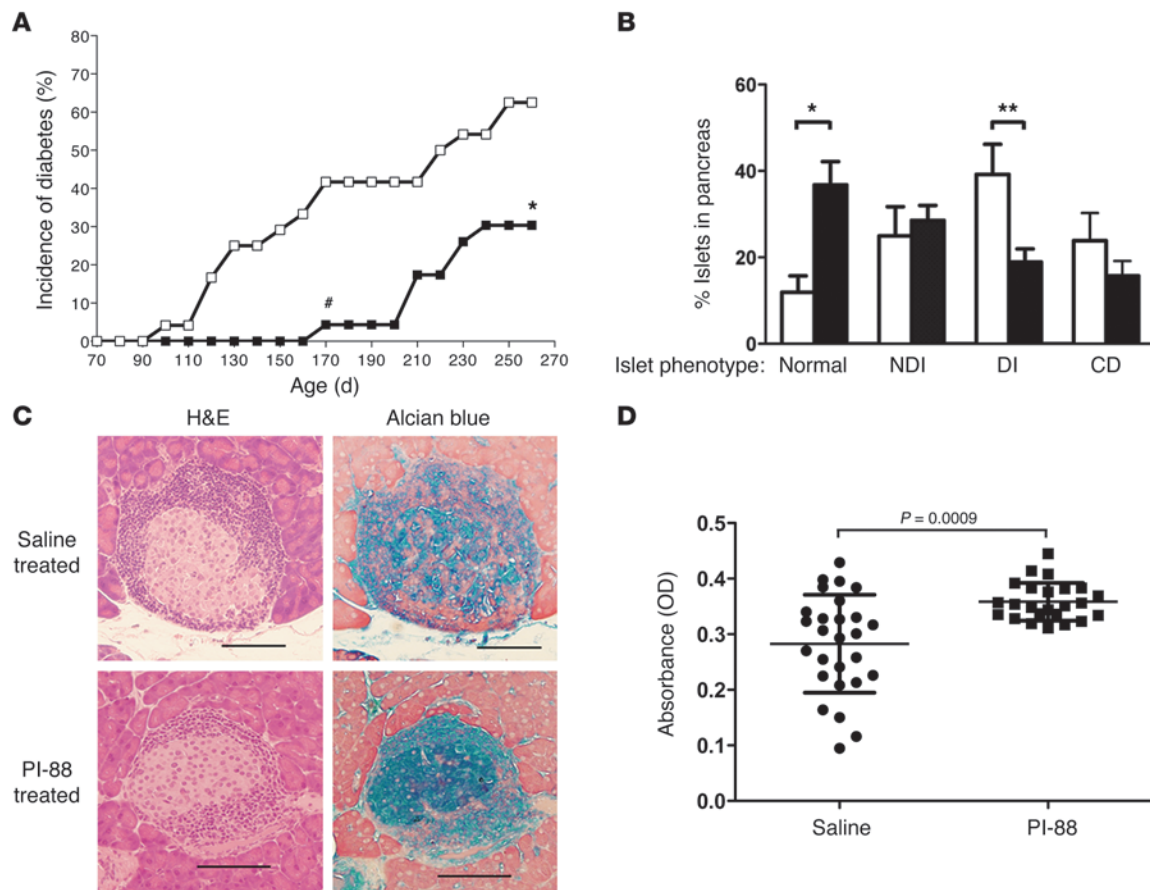
Figure 3
Enzymatically active heparanase is expressed by DI MNCs in NOD mice. (**A**) H&E and Alcian blue staining of NOD/Lt islets demonstrated that intact islets without insulitis (I) or islets with NDI contained extensive HS. In contrast, DI (arrow) was associated with local disruption of islet HS (asterisks). Scale bars: 100 μm. (**B**) Quantification of islet area stained by Alcian blue showed a significant reduction in islet-associated HS in prediabetic (PD) and onset-diabetic (OD) NOD/Lt mice compared with NOD/SCID (Sc) mice. Y, young 4- to 5-week-old NOD/Lt donors. $n = 60–70$ islets/group, 6–7 pancreases/group. Data are mean ± SEM. *$P < 0.001$. (**C**) Stereomacroscopic view of prediabetic NOD/Lt islets showing a clear, well-defined boundary of an intact islet and islets with insulitis, indicated by a translucent appendage of insulitis MNCs (arrows). (**D**) *Hpse* and (**E**) *Cd45* transcript expression in isolated islets, expressed relative to CBA/H kidney (K) and NOD/SCID islets, respectively. N, normal CBA/H donors. Results are mean ± SD ($n = 3$ per group). *$P < 0.0001$. (**F**) Heparanase immunohistochemistry showed strong expression of heparanase protein by DI MNCs in a diabetes-onset NOD/Lt pancreas (HP130 mAb). Note weak cell surface expression of heparanase (arrows) on NOD/SCID and diabetes-onset NOD/Lt islet cells. Scale bars: 100 μm. (**G**) Western blot analysis of mouse proheparanase (prohpse; 1453 pAb; 65 kDa) and active heparanase (hpse; HP130 mAb; 48 kDa) in protein extracts from pooled islets (10 donors/group). Heparanase (50 ng) purified from human platelets (Hu Hpse) was included as a 50-kDa standard.

10 weeks, and the proportion of mice with diabetes at 36 weeks of age was reduced by 50% (Figure 4A). At the end of the experiment, islets in the pancreas from PI-88–treated and saline-treated nondiabetic mice were examined to assess the level of insulitis. Compared with saline-treated controls, PI-88–treated mice showed a significant increase in the proportion of islets showing no insulitis, and the proportion of islets with DI was significantly decreased (Figure 4B). Islets with DI from PI-88–treated mice also showed significantly better preservation/restoration of islet-associated HS than islets from control saline-treated mice, in which Alcian blue staining demonstrated that DI was associated with extensive fragmentation and loss of islet HS (Figure 4, C and D). In fact, the intensity of HS staining in islets from PI-88–treated mice was significantly higher (~1.3-fold)

and less variable than for islets from saline-treated mice (Figure 4D). Overall, compared with the saline-treated controls, which developed T1D, PI-88 treatment completely protected 50% of clinical disease–prone NOD/Lt mice from T1D (with significantly improved islet pathology and islet HS) and significantly delayed T1D onset in the remainder. These results support the notion that heparanase critically contributes to T1D development by inhibiting islet invasion by insulitis MNCs and subsequent loss of intra-islet HS.

Discussion

We report here that pancreatic β cells have a uniquely abundant intracellular store of HS, which plays a role in β cell survival that we believe to be previously unrecognized. During islet

Figure 4

Inhibition of heparanase activity in vivo protects NOD mice from T1D and destructive immunity. (**A**) NOD/Lt female mice (10.5–11 weeks) were injected daily i.p. with 10 mg/kg PI-88 (black; $n = 23$ per group) or saline (white; $n = 25$ per group). PI-88 treatment delayed the onset of diabetes by 70 days and reduced the incidence of diabetes to 30% compared with 62% in control mice. #$P = 0.0039$, *$P = 0.0415$ vs. saline. (**B**) Pancreases from nondiabetic PI-88– (black; $n = 4$ per group) or saline-treated (white; $n = 3$ per group) NOD/Lt mice at 253 days of age (from **A**) were analyzed histologically to assess the level of insulitis. PI-88 treatment significantly increased the percentage of islets lacking insulitis (normal) and significantly decreased the percentage of islets with DI, with a noticeable reduction also observed in completely destroyed (CD) islets. Results are mean ± SEM. *$P = 0.0026$; **$P = 0.0244$. (**C**) Additional serial pancreas sections from **B** were alternately stained with H&E and Alcian blue. PI-88 treatment preserved islet-associated HS in the presence of DI, compared with control islets from saline-treated mice, in which intraislet HS was severely disrupted. Scale bars: 100 μm. (**D**) Alcian blue staining intensity was significantly stronger in islets with DI from PI-88–treated mice than from control saline-treated mice from **B** ($P = 0.0009$), as quantified by Image J with Color Deconvolution plugin. Results are mean ± SD.

isolation, approximately 50% of the islet HS content was lost, and during culture of isolated β cells, there was a progressive decline in intracellular HS that correlated with increased β cell apoptosis and death. Surprisingly, HS replacement — achieved by culturing β cells with the highly sulfated HS analog heparin and confirmed by uptake of FITC-labeled heparin — rescued the β cells from apoptosis and dramatically improved β cell survival. Furthermore, the transition from calcein+PI+ apoptotic β cells to calcein+PI– viable cells was confirmed by loss of staining with 7-amino-actinomycin D (7AAD), a DNA-binding dye conventionally used for identifying apoptotic cells (data not shown). Rescue by HS replacement with heparin, HShi, or PI-88 not only prevented culture-induced cell death, but also rendered the β cells remarkably resistant to death induced by free radicals (i.e., ROS), which suggests that β cell death in vitro may be mediated by excessive levels of free radicals produced endogenously in the β cells. Overall, these findings suggest that in situ, normal

levels of endogenous intracellular HS may function, at least in part, to protect β cells from free radical–induced cell injury.

Heparin imported into β cells in vitro and endogenous β cell HS in situ (i.e., in the pancreas) may interact directly with ROS and function as an antioxidant or free radical sink (34–36). The depolymerization of HS by free radical species, for example, could represent an antioxidant mechanism for protecting β cells from free radical damage. In vitro, exposure of rat glomerular BM HS to ROS generated by hypoxanthine/xanthine oxidase reactions results in HS fragmentation or depolymerization, detected by PAGE (34). Similarly, hydroxyl radicals have previously been shown to efficiently depolymerize heparin to low–molecular weight heparins (35). Alternatively, free radicals may be chemically detoxified by removing the anomeric hydrogen of internal sugar residues of HS, as previously reported for polyelectrolyte configurations of glucose, such as phosphorylated or sulfated glucans (36). Unlike depolymerization, a role for HS as a free radical sink would be

expected to better preserve other biological functions of the HS chains. β cells are highly metabolically active and consequentially generate considerable levels of intracellular ROS via disulfide bond formation during insulin biosynthesis in the endoplasmic reticulum or during oxidative phosphorylation or disulfide bond formation for protein folding in mitochondria (37, 38). β cell HS could therefore provide a constitutive mechanism for detoxifying endogenous ROS and thereby compensate for the reported low levels of free radical scavenger enzymes in β cells (18).

We found that inadvertent depletion of intracellular HS during isolation of islets and β cells in vitro rendered β cells particularly vulnerable to damage induced by exogenously delivered ROS and that HS replacement via treatment of β cells with heparin or other HS mimetics in culture provided resistance to ROS. Islets have been reported to undergo matrix detachment-induced apoptosis (anoikis) during their enzyme-mediated isolation (39, 40), and this process in epithelial cells correlates with ROS induction (41). Taken together, these properties suggest a scenario in which, during islet/β cell isolation, islets undergo matrix detachment that substantially elevates endogenous ROS levels in β cells to levels exceeding the protective capabilities of HS, resulting in HS degradation and apoptosis. We further speculate that providing additional excessive exogenous ROS (by acute treatment with H_2O_2) at this time may precipitate β cell apoptosis and death. Like β cells, apoptosis induced in rat kidney glomerular mesangial cells by chronic treatment with H_2O_2 for 24 hours was prevented by pretreatment with heparin or HSPG. Explant-induced apoptosis of glomerular cells was similarly protected by acute treatment with heparin in vitro (42), and we speculate that this early damage may also be attributable to matrix detachment. Furthermore, ultra–low–molecular weight heparin has been reported to prevent glutamate-induced apoptosis in brain cortical cells in vitro and to prevent free radical–induced damage after ischemia/reperfusion injury in rat brain in vivo (43, 44). Our demonstration that HS replacement by heparin rescued β cells from free radical damage and apoptosis in vitro is consistent with these prior reports and with the notion that islets/β cells in situ express exceptionally high levels of endogenous HS in order to execute similar prosurvival functions in vivo. Apoptosis in β cells is attributed to imbalanced expression of pro- and antiapoptotic genes of the Bcl-2 family (45–47), which suggests that HS may also function in regulating gene expression in β cells, as previously reported for other cell types (48, 49). In any case, our findings strongly implicate HS preservation during human islet isolation or HS replacement as strategies for improving islet viability and for reducing the number of islets (and donors) required for clinical islet transplantation as a treatment for established T1D.

In addition to playing a critical role in β cell survival, HS may also perform other homeostatic functions as a reservoir and coreceptor for essential growth factors (50) and has previously been reported to regulate the postnatal development of β cell function (26). Under conditions of autoimmune disease, we demonstrated here that islet HS acts as a critical target for destruction by heparanase. This finding builds on our earlier observation that islets are surrounded by a continuous BM containing the HSPG perlecan, with MNC entry into the islets during destructive autoimmunity being accompanied by degradation of perlecan in the islet BM (19). Thus, DI MNCs produce catalytically active heparanase that — by solubilizing the islet BM HS — allows intra-islet MNC invasion, induces β cell death, and initiates autoimmune diabetes. Paradoxically, we

also showed that islet β cells endogenously produced heparanase, which probably has a homeostatic function in regulating the turnover of HS (50) and possibly gene expression (48, 49).

Overall, our data are completely consistent with the idea that T1D is heparanase dependent, since T1D is an autoimmune disease mediated by insulitis MNCs, PI-88 efficiently inhibited heparanase, and PI-88 treatment altered autoimmune-associated pathology in NOD mice. Although the drug can also disrupt interactions between HS and certain growth factors (27), this secondary role is unlikely to enhance β cell survival. In further support of a causal role for heparanase in T1D, we also found that more specific heparanase inhibitors that have minimal growth factor binding and anticoagulant activity were as effective as PI-88 at protecting approximately 50% of NOD mice from developing T1D (data not shown). Heparanase may nevertheless affect T1D development at multiple sites. First, heparanase is likely to function at the level of facilitating MNC migration across the subvascular endothelial BM in the pancreas (20) and, possibly, subsequent passage through the ECM of the pancreas. Secondly, at the level of the islet microenvironment, we propose that the production of catalytically active heparanase by insulitis MNCs and degradation of islet BM HS signals the onset of destructive autoimmunity. Thereafter, migration of insulitis MNCs into the targeted islets results in local intraislet production of active heparanase, progressive loss of β cell HS, β cell apoptosis, loss of insulin production, β cell death, and ultimately T1D. Likewise, PI-88–mediated inhibition of heparanase could therefore inhibit T1D development at each tier of heparanase involvement. However, long-term treatment of NOD mice with PI-88 resulted in a significant increase in the percentage of intact islets (without insulitis) and a significant decrease in the percentage of islets with DI (Figure 4B), suggestive of drug-mediated protection occurring at both vascular and peri-islet sites.

Heparanase has previously been shown to function in disease by regulating BM breakdown and ECM remodeling via HS degradation. These actions facilitate cell migration in inflammation, spread of metastatic tumor cells and their reestablishment as solid tumors at secondary sites, and glomerular BM degeneration in diabetic nephropathy (29, 51, 52). In addition to these more standard functions, our present study identified that heparanase produced by insulitis MNCs plays a direct and fundamental role as an effector mechanism in T1D by degrading β cell HS, a process that leads to β cell death. Our findings unveil a critical role for islet HS in β cell survival and highlight the potential for new therapeutic approaches for rescuing β cell function at the time of T1D onset by HS replacement therapy, as well as for blocking progressive loss of islet-associated HS during disease development with heparanase inhibitors, both of which could be achieved using appropriately designed HS mimetics.

Methods

Further information can be found in Supplemental Methods.

Mice and T1D monitoring. Specific pathogen–free female NOD/Lt mice (4–5 weeks old) were obtained from the Animal Resource Centre (Perth, Australia), and other strains were obtained from the Animal Services Division of The John Curtin School of Medical Research or The Australian National University Bioscience Facility (Canberra, Australia). Onset of clinical diabetes was determined by measuring urine glucose twice weekly with Multistix reagent strips (Bayer) and confirmed by measuring nonfasting blood glucose levels in tail vein blood using a MediSense glucometer (Abbott Laboratories). Hyperglycemia was defined in our study as 2 consecutive blood glucose readings of 16 mmol/l or greater.

In vivo treatment of prediabetic NOD/Lt mice with PI-88. We treated NOD/Lt female mice at 10.5–11 weeks of age daily for 180 days by i.p. injection with 10 mg/kg PI-88 (provided by Progen Pharmaceuticals) or with 8 μl/g saline diluent.

Islet isolation. Islets were isolated as previously described (53, 54). Briefly, islets were isolated from anesthetized donor mice (Avertin, 0.025 ml/g body weight) by initially perfusing the pancreas in situ via the pancreatic duct with 2.5 mg/ml collagenase P (Roche Diagnostics). The distended pancreas was digested further with an additional 2.5 mg/ml collagenase P in a stationary water bath at 37°C. The digested tissue was then briefly shaken, vortexed lightly, placed on ice to terminate enzymatic digestion, and subsequently washed 3 times. Islets were hand-picked from the digested pancreas tissue with the aid of a dissecting microscope (Kyowa Optical SDZ-P). For isolation of islets from prediabetic and diabetes-onset NOD/Lt donors, an inverted microscope (Olympus CK) was also used to help distinguish islets with insulitis from dissociated acinar tissue. We photographed islets showing attached insulitis using an inverted microscope (Leica Microsystems).

Preparation and culture of isolated β cells. We dispersed BALB/c mouse islets into single-cell suspensions using the method of Josefsen et al. (55), modified to use 1 mg/ml Dispase II (Roche) in the chelation buffer, and subsequently cultured the islet cells on uncoated plastic. The cells were cultured at $2.5–4 \times 10^4$ cells/well in CELLSTAR 96-well plates (Greiner Bio-one) in RPMI 1640 medium (Gibco; Invitrogen), supplemented with 10% fetal calf serum (SAFC Biosciences), in the presence or absence of heparin from bovine lung (Sigma-Aldrich) or porcine intestinal mucosa (Celsus Laboratories), PI-88 (provided by Progen Pharmaceuticals), porcine mucosal HS[hi] (HI-11098; Celsus Laboratories) or HS[lo] (HO-10595; Celsus Laboratories) at 0.5–50 μg/ml for 1 hour to 2 days in 5% CO_2, 95% air, at 37°C. During culture, the isolated β cells adhered to the hydrophilic tissue culture-treated plastic surface of the wells in the culture plates. β cells were treated with 30% H_2O_2 (Chem-Supply) for 5 minutes at 37°C as a source of ROS and were used as a positive control for analysis of β cell death on day 0.

Flow cytometry. We assessed cell death by incubating β cells with 31.25 nM Sytox green (Invitrogen) for 15 minutes at 37°C. The region identifying dead cells was defined using H_2O_2-treated cells as positive controls. Cell viability was also analyzed by staining initially with calcein-AM (0.04 μM; Invitrogen) and subsequently with propidium iodide (PI; 2.5 μg/ml; BD Biosciences – Pharmingen), each for 15 minutes at 37°C. Viable cells were identified as calcein[+]PI[–], apoptotic cells as calcein[+]PI[+], and dead cells as calcein[–]PI[+]. When PI was replaced with 7AAD (10 μg/ml; Molecular Probes) in the presence of calcein, a similar proportion of apoptotic cells was observed. 10E4 and HepSS-1 mouse mAbs (Seikagaku), sheep anti-mouse Ig-R–phycoerythrin (Chemicon) or goat anti-mouse Ig-R–phycoerythrin (Southern Biotech), BD Cytofix/Cytoperm Fixation/Permeabilization Kit (BD Biosciences – Pharmingen), and mouse IgM (BD Biosciences – Pharmingen) as isotype control were used for HS staining of β cells, gated for viability using forward and side scatter properties. Flow-Count Fluorospheres (Beckman Coulter) were added (4,000 beads/cell sample) prior to staining to determine cell numbers. The geometric mean fluorescence intensity ratio (GMFR) was calculated by dividing the geometric mean fluorescence intensity of cells stained with primary Ab by that of cells stained with the isotype control. Cells were analyzed using a BD LSRI flow cytometer and CellQuest software (version 6.0, BD Biosciences).

Western blotting. Islets were lysed in 1% CHAPS (3-[{3-cholamidopropyl}dimethylammonio]-1-propanesulfonate; Sigma-Aldrich) containing 50 mM EDTA, 50 μM E64 (Sigma-Aldrich), 1 mg/ml Pefabloc SC (Roche Diagnostics), and Complete Protease Inhibitor Cocktail Tablets (EDTA-free, at ×20 recommended concentration; Roche Diagnostics) at pH 8.0. The protein concentration of islet lysates was measured using

Bio-Rad protein Dye Reagent (Bio-Rad Labs). Lysates (300 μg/sample) were incubated with concanavalin A–sepharose beads (Pharmacia) for 2 hours, washed, and then boiled in reducing buffer prior to SDS-PAGE. Marker proteins (Precision Plus Protein Standards, Dual Color; Bio-Rad) and 50 ng purified human platelet heparanase (56) were run in parallel. Nitrocellulose membranes were probed with HP130 mAb (Insight Biopharmaceuticals) or affinity-purified rabbit anti–recombinant human proheparanase polyclonal Ab 1453 (provided by I. Vlodavsky, Rappaport Faculty of Medicine, Technion, Haifa, Israel) (57) followed by HRP-conjugated rabbit anti-mouse Ig (Dako) or HRP-conjugated swine anti-rabbit Ig (Dako). Immunoreactive proteins were detected using ECL Western Blotting Reagent (Amersham) and a LAS-1000 Chemiluminescence and Fluorescence Imaging System (Fuji Photo Film).

Real-time PCR. For analysis of heparanase, CD45, and ubiquitin conjugating enzyme E2D1 (UBC; endogenous reference gene) transcripts in isolated islets, we used validated TaqMan real-time gene expression assays (Applied Biosystems, catalog nos. Mm00461768_m1, Mm00448463_m1, and Mm00461037_g1). The mean Ct values for UBC between experimental groups were 27.6–29.9. Quantification of changes in transcript expression was calculated using the comparative Ct method as previously described (58), which corrects for any variation between samples in template input by normalization to the endogenous reference gene.

Histology and immunohistochemistry. Pancreas and islet samples were fixed in 10% neutral-buffered formalin, and paraffin sections (4 μm) were prepared. Sections were stained with H&E or with Alcian blue (0.65 M $MgCl_2$, pH 5.8; Sigma-Aldrich) for selective identification of HS glycosaminoglycans (refs. 23, 59, and Supplemental Figure 1) and counterstained using safranin. For quantitative studies of NOD/Lt islet integrity, 8 H&E-stained semiserial sections of each pancreas specimen (minimum interval of 48 μm between sections analyzed) were examined by 2 observers in a blinded fashion, and the percentage of islets with each descriptor (normal, NDI, DI, or completely destroyed) were quantified and expressed as mean ± SEM of the total islets counted in the pancreas sections. Image J software (version 1.44a; NIH) with Color Deconvolution plugin (60) was used to quantify the intensity of Alcian blue staining. For measurement of the intensity (optical density), images were deconvoluted using the plugin to separate the Alcian blue staining component from the counterstain safranin. The mean optical density of Alcian blue staining was then determined by converting the mean pixel value for islet tissue (including insulitis) to optical density, using the calculation $\log_{10}(255/\text{mean pixel value})$. For analysis of islets from saline- and PI-88–treated NOD/Lt mice, 3 sections per specimen were analyzed for 3 (saline) or 4 (PI-88) specimens, with the minimum interval between sections analyzed being 48 μm. For assessment of area of Alcian blue staining, BALB/c islets in situ ($n = 50$ from 4 pancreas specimens; 1 section/specimen), BALB/c islets after isolation ($n = 45$ from 3 pooled islet specimens; 1 section/specimen), and NOD/Lt islets in situ at different stages of autoimmune disease and NOD/SCID islets in situ ($n = 6–7$ pancreas specimens/group; 3 sections/specimen) were analyzed, with the minimum interval between sections analyzed being 64 μm. We localized HS (10E4 or HepSS-1 mAbs) and heparanase (HP-130 mAb) by immunohistochemistry after antigen retrieval using 0.05% pronase protease (Calbiochem) for HS (61) or heat-induced standard antigen retrieval for heparanase (62), using the M.O.M. immunodetection kit (Vector Laboratories). Control sections were incubated with isotype control Ig.

Statistics. For statistical analyses of differences between groups, we used 2-tailed, unpaired Student's *t* test, Mann-Whitney test, or ANOVA with Kruskal-Wallis post-test for histological analyses; Mann-Whitney test for real-time PCR analyses; Fisher exact test for cumulative incidence of diabetes; and Student's *t* test, Mann-Whitney test, or ANOVA with Bonferroni post-test for flow cytometry data analyses. A *P* value less than 0.05 was considered statistically significant.

1. Solomon M, Sarvetnick N. The pathogenesis of diabetes in the NOD mouse. *Adv Immunol*. 2004; 84:239–264.
2. Kägi D, Odermatt B, Seiler P, Zinkernagel RM, Mak TW, Hengartner H. Reduced incidence and delayed onset of diabetes in perforin-deficient Non-Obese Diabetic mice. *J Exp Med*. 1997;186(7):989–997.
3. Mathis D, Vence L, Benoist C. β-cell death during progression to diabetes. *Nature*. 2001; 414(6865):792–798.
4. Allison J, Thomas HE, Catterall T, Kay TW, Strasser A. Transgenic expression of dominant negative Fas-associated death domain protein in β cells protects against Fas ligand-induced apoptosis and reduces spontaneous diabetes in nonobese diabetic mice. *J Immunol*. 2005;175(1):293–301.
5. Chervonsky A, et al. The role of Fas in autoimmune diabetes. *Cell*. 1997;89(1):17–24.
6. Estella E, et al. Granzyme B-mediated death of pancreatic beta-cells requires the proapoptotic BH3-only molecule bid. *Diabetes*. 2006;55(8):2212–2219.
7. Mallone R, Brezar V, Boitard C. T cell recognition of autoantigens in human Type 1 diabetes: Clinical perspectives. *Clin Dev Immunol*. 2011;2011:513210.
8. Koike T, et al. Preventive effect of monoclonal anti-L3T4 antibody on development of diabetes in NOD mice. *Diabetes*. 1987;36(4):539–541.
9. Shizuru JA, Taylor-Edwards C, Banks BA, Gregory AK, Fathman CG. Immunotherapy of the nonobese diabetic mouse: treatment with an antibody to T-helper lymphocytes. *Science*. 1988;240(4852):659–662.
10. Chatenoud L, Thervet E, Primo J, Bach JF. Anti-CD3 antibody induces long-term remission of overt autoimmunity in nonobese diabetic mice. *Proc Natl Acad Sci U S A*. 1994;91(1):123–127.
11. Meagher C, et al. Neutralization of interleukin-16 protects nonobese diabetic mice from autoimmune type 1 diabetes by a CCL4-dependent mechanism. *Diabetes*. 2010;59(11):2862–2871.
12. McGuire HM, et al. Interleukin-21 is critically required in autoimmune and allogeneic responses to islet tissue in murine models. *Diabetes*. 2011; 60(3):867–875.
13. Chee J, et al. TNF receptor 1 deficiency increases regulatory T cell function in nonobese diabetic mice. *J Immunol*. 2011;187(4):1702–1712.
14. Bouma G, et al. Evidence for an enhanced adhesion of DC to fibronectin and a role of CCL19 and CCL21 in the accumulation of DC around the prediabetic islets in NOD mice. *Eur J Immunol*. 2005; 35(8):2386–2396.
15. Martin AP, et al. Islet expression of M3 uncovers a key role for chemokines in the development and recruitment of diabetogenic cells in NOD mice. *Diabetes*. 2008;57(2):387–394.
16. Lin G-J, et al. Transgenic expression of murine chemokine decoy receptor D6 by islets reveals the role of inflammatory CC chemokines in the development of autoimmune diabetes in NOD mice. *Diabetologia*. 2011;54(7):1777–1787.

17. Couzin-Frankel J. Trying to reset the clock on Type 1 Diabetes. *Science*. 2011;333(6044):819–821.
18. Tiedge M, Lortz S, Drinkgern J, Lenzen S. Relation between antioxidant enzyme gene-expression and antioxidant defense status of insulin-producing cells. *Diabetes*. 1997;46(11):1733–1742.
19. Irving-Rodgers H, et al. Molecular composition of the peri-islet basement membrane in NOD mice: a barrier against destructive insulitis. *Diabetologia*. 2008; 51(9):1680–1688.
20. Parish CR. The role of heparan sulfate in inflammation. *Nat Rev Immunol*. 2006;6(9):633–643.
21. Esko JD, Selleck SB. Order out of chaos: Assembly of ligand binding sites in heparan sulfate. *Ann Rev Biochem*. 2002;71:435–471.
22. Vlodavsky I, Friedmann Y. Molecular properties and involvement of heparanase in cancer metastasis and angiogenesis. *J Clin Invest*. 2001;108(3):341–347.
23. Scott JE, Dorling J. Differential staining of acid glycosaminoglycans (muco-polysaccharides) by alcian blue in salt solutions. *Histochemie*. 1965;5(3):221–233.
24. Oldberg A, Höök M, Obrink B, Pertoft H, Rubin K. Structure and metabolism of rat liver heparan sulfate. *Biochem J*. 1977;164(1):75–81.
25. Lindahl U, Bäckstrom G, Jansson L, Hallén A. Biosynthesis of heparin. II. Formation of sulfamino groups. *J Biol Chem*. 1973;248(20):7234–7241.
26. Takahashi I, et al. Important role of heparan sulfate in postnatal islet growth and insulin secretion. *Biochem Biophys Res Commun*. 2009;383(1):113–118.
27. Parish CR, Freeman C, Brown KJ, Francis DJ, Cowden WB. Identification of sulfated oligosaccharide-based inhibitors of tumor growth and metastasis using novel in vitro assays for angiogenesis and heparanase activity. *Cancer Res*. 1999; 59(1):3433–3441.
28. Ferro V, et al. PI-88 and novel heparan sulfate mimetics inhibit angiogenesis. *Semin Thromb Hemost*. 2007;33(5):557–568.
29. Parish CR, Freeman C, Hulett MD. Heparanase: a key enzyme involved in cell invasion. *Biochim Biophys Acta*. 2001;1471(3):M99–M108.
30. Fairbanks MB, et al. Processing of the human heparanase precursor and evidence that the active enzyme is a heterodimer. *J Biol Chem*. 1999; 274(42):29587–29590.
31. Hulett MD, Freeman C, Hamdorf BJ, Baker RT, Harris MJ, Parish CR. Cloning of mammalian heparanase, an important enzyme in tumor invasion and metastasis. *Nat Med*. 1999;5(7):803–809.
32. Vlodavsky I, et al. Mammalian heparanase: gene cloning, expression, and function in tumor progression and metastasis. *Nat Med*. 1999;5(7):793–802.
33. Lewis KD, et al. A phase II study of the heparanase inhibitor PI-88 in patients with advanced melanoma. *Invest New Drugs*. 2008;26(1):89–94.
34. Raats CJ, Bakker MA, van den Born J, Berden JHM. Hydroxyl radicals depolymerize glomerular heparan sulfate in vitro and in experimental nephritic syndrome. *J Biol Chem*. 1997;272(42):26734–26741.

35. Rota C, et al. Free radical generation during chemical depolymerization of heparin. *Anal Biochem*. 2005;344(2):193–203.
36. Tsiapali E, Whaley S, Kalbfleisch J, Ensley HE, Browder IW, Williams DL. Glucans exhibit weak anti-oxidant activity, but stimulate macrophage free radical activity. *Free Rad Biol Med*. 2001; 30(4):393–402.
37. Yuan Y, Wang ZH, Tang JG. Intra-A chain disulphide bond forms first during insulin precursor folding. *Biochem J*. 1999;343 pt 1:139–144.
38. Riemer J, Bulleid N, Herrmann JM. Disulfide formation in the ER and mitochondria: Two solutions to a common process. *Science*. 2009; 324(5932):1284–1287.
39. Thomas FT, Contreras JL, Bilbao G, Ricordi C, Curiel D, Thomas JM. Anoikis, extracellular matrix, and apoptosis factors in isolated cell transplantation. *Surgery*. 1999;126(2):299–304.
40. Wang RN, Rosenberg L. Maintenance of β cell function and survival following islet isolation requires re-establishment of the islet-matrix relationship. *J Endocrinol*. 1999;163(2):181–190.
41. Schafer ZT, et al. Antioxidant and oncogene rescue of metabolic defects caused by loss of matrix detachment. *Nature*. 2009;461(7260):109–113.
42. Yoshihisa I, Kitamura M. Inhibition of glomerular cell apoptosis by heparin. *Kidney Int*. 1999; 56(3):954–963.
43. Zhang ZG, Zhang QZ, Cheng YN, Ji SL, Du GH. Antagonistic effects of ultra-low-molecular weight heparin against cerebral ischemia/reperfusion injury in rats. *Pharmacol Res*. 2007;56(4):350–355.
44. Yu TG, Zhang QZ, Zhang ZG, Wang WW, Ji SL, Du GH. Protective effect of ultra low molecular weight heparin on glutamate-induced apoptosis in cortical cells. *Yonsei Med J*. 2008;49(3):486–495.
45. Thomas HE, McKenzie MD, Anstera E, Campbell PD, Kay T. β cell apoptosis in diabetes. *Apoptosis*. 2009; 14(12):1389–1404.
46. Gurzov EN, et al. Signaling by IL-1β + IFN-γ and ER stress converge on DP5/Hrk activation: a novel mechanism for pancreatic β-cell apoptosis. *Cell Death Differ*. 2009;16(11):1539–1550.
47. Allagnat F, Cunha D, Moore F, Vanderwinden JM, Eizirik DL, Cardozo AK. Mcl-1 downregulation by proinflammatory cytokines and palmitate is an early event contributing to β-cell apoptosis. *Cell Death Differ*. 2011;18(2):328–337.
48. Kobayashi M, Naomoto Y, Nobuhisa T. Heparanase regulates esophageal keratinocyte differentiation through nuclear translocation and heparan sulfate cleavage. *Differentiation*. 2006;74(5):235–243.
49. Buczek-Thomas JA, Hsia E, Rich CB, Foster JA, Nugent MA. Inhibition of histone acetyltransferase by glycosaminoglycans. *J Cell Biochem*. 2008; 105(1):108–120.
50. Bernfield M, et al. Functions of cell surface heparan sulfate proteoglycans. *Ann Rev Biochem*. 1999; 68:729–777.

51. Vlodavsky I, et al. Significance of heparanase in cancer and inflammation [published online ahead of print August 3, 2011]. *Cancer Microenviron.* doi:10.1007/s12307-011-0082-7.

52. van den Hoven MJ, Rops AL, Vlodavsky I, Levidiotis V, Berden JH, van der Vlag J. Heparanase in glomerular diseases. *Kidney Int.* 2007;72(5):543–548.

53. Gazda LS, Charlton B, Lafferty KJ. Diabetes results from a late change in the autoimmune response of NOD mice. *J Autoimmunity.* 1997;10(3):261–270.

54. Simeonovic CJ, Zarb JC, Gazda LS, Lafferty KJ, Wilson JD. Pancreatic islet and proislet transplantation in the mouse model. In: Timmermann W, Ulrichs K, Thiede DA, eds. *Microsurgical Models in Rats and Mice for Transplantation Research.* Berlin: Springer-Verlag; 1998:167–77.

55. Josefsen K, et al. Fluorescence-activated cell sorted rat islet cells and studies of the insulin secretory process. *J Endocrinol.* 1996;149(1):145–154.

56. Freeman C, Parish CR. Human platelet heparanase: purification, characterization and catalytic activity. *Biochem J.* 1998;330(pt 3):1341–1350.

57. Zetser A, et al. Processing and activation of latent heparanase occurs in lysosomes. *J Cell Science.* 2004; 117(pt 11):2249–2258.

58. Popp SK, et al. Transient transmission of porcine endogenous retrovirus to fetal lambs after pig islet tissue xenotransplantation. *Immunol Cell Biol.* 2007; 85(3):238–248.

59. Calvitti M, et al. Bronchial branching correlates with specific glycosidase activity, extracellular glycosaminoglycan accumulation, TGFbeta(2), and IL-1 localization during chick embryo lung development. *J Histochem Cytochem.* 2004;52(3):325–334.

60. Ruifrok AC, Johnston DA. Quantification of histochemical staining by color deconvolution. *Anal Quant Cytol Histol.* 2001;23(4):291–299.

61. Frevert CW, et al. Binding of Interleukin-8 to heparan sulfate and chondroitin sulfate in lung tissue. *Am J Respir Cell Mol Biol.* 2003;28(4):464–472.

62. Joyce JJ, Freeman C, Meyer-Morse N, Parish CR, Hanahan DA. A functional heparan sulfate mimetic implicates both heparanase and heparan sulfate in tumor angiogenesis and invasion in a mouse model of multistage cancer. *Oncogene.* 2005;24(25):4037–4051.